3386 © *1984 The Chemical Society of Japan* *Bull. Chem. Soc. Jpn., 57, 3386—3390 (1984)* [Vol. 57, No. 12

A Study of the Charge-Discharge Characteristics of the Lithium–Polyacetylene Battery by Means of the FFT Impedance Measurement

Tetsuya Osaka* and Takashi Kitai
Department of Applied Chemistry, School of Science and Engineering, Waseda University,
Okubo, Shinjuku-ku, Tokyo 160

(Received March 13, 1984)

The charge-discharge characteristics of the anion-doped lithium-polyacetylene [$(CH)_x$] battery was investigated by means of the FFT impedance method, by which the impedance-frequency dispersion could be measured by very high speed. The charging and self-discharging of the Li-$(CH)_x$ battery were represented by the Randles-type equivalent circuit, added with the corrective term concerned with surface roughness. These processes and their doping states of the $(CH)_x$ film were readily detected by the variation in the resistive component, *Rr*, in the equivalent circuit. The *Rr* value of the self-discharge process was clearly correlated to the open-circuit voltage, *Voc,* regardless of the charging current; furthermore, it was strongly indicated that the self-discharge process is mainly caused by the dopant diffusion from the interface into the interior part of $(CH)_x$ films. For the discharging process, another mechanism, closely concerned with dopant diffusion, was suggested by the impedance results.

The electrochemical doping-undoping method in polyacetylene has been of much interest when applied for lightweight rechargeable batteries.[1,2] The MacDiarmid group[1] indicated the high potential on rechargeable battery by using 6% ClO_4^- doped polyacetylene as a cathode-active material. Moreover, they[2] summarized some characteristics of the lithium–polyacetylene battery in which 7% doped polyacetylene was used as the cathode. The electrochemical doping-undoping processes of polyacetylene have already been studied by FFT impedance measurement[3] and the basic doping-undoping process could readily be analysed by means of the resistive component measured by the FFT impedance measurement at a high speed. In this paper, we wish to report the charge-discharge and self-discharge characteristics of the ClO_4^- doped lithium–polyacetylene battery as established by means of electrochemical measurements, especially by the FFT impedance method.[4]

Experimental

The *cis*-polyacetylene films 0.1 mm thick (weight density, 0.44 g cm^{-3}) were prepared by the Sirakawa method.[5] The cell construction, composed of 8 mmϕ *cis*-$(CH)_x$ working and Li counter electrodes attached to platinum plates, without any reference electrode, is shown schematically in Fig. 1. The volume of the cell was 0.283 cm^3. The polyacetylene working and lithium counter electrodes were fixed by the use of stainless steel SUS 304 fittings with O-rings for sealing. One mol dm^{-3} $LiClO_4$ electrolyte and propylene carbonate (PC) were purified and handled in the usual method.[6] The Li-*p*-$(CH)_x$ battery was galvanostatically charged or discharged using the step-by-step or the consecutive method. The doping level of the $(CH)_x$ film was calculated according to Eq. 1; one percent of the doping level for the film corresponded to 278 mC. The doping was carried out conveniently until the 6% level was reached by referring the Refs. 1 and 2 in order to avoid the irreversible oxidation of the $(CH)_x$ film. The cell impedance was measured from 0.001 to 2.5 kHz by means of the on-line FFT impedance meter constructed by the authors' laboratory.[4] All the experiments were carried out in a dry and inert Ar gas atmosphere.

Results and Discussion

Open-circuit Voltage, Voc, *on Charging-Discharging Process of ClO_4^- Doped Li-$(CH)_x$ Battery.* The relations between the open-circuit voltage, *Voc,* and the doping level, *y,* for the step-by-step charging-discharging process of lithium/1 mol dm^{-3} $LiClO_4$ in the propylene carbonate/$(CH)_x$ battery have already been reported by several workers.[1,2] The basic charging process for the ClO_4^- anion doping into the $(CH)_x$ film is represented by:

$$(CH)_x + xyClO_4^- \longrightarrow [CH^{y+}(ClO_4^-)_y]_x + xye. \quad (1)$$

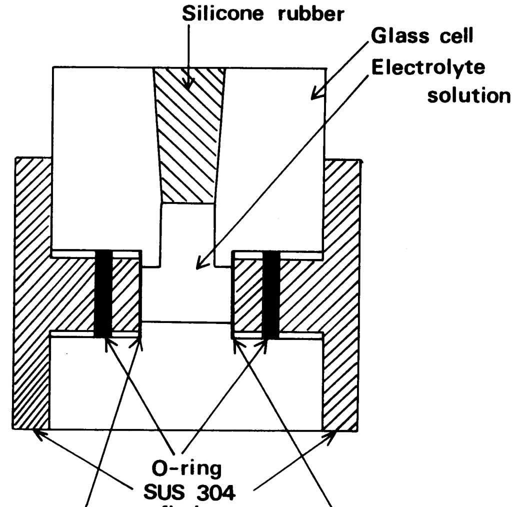

Fig. 1. Schematic cell construction of Li/1 mol dm^{-3} in PC/$(CH)_x$.

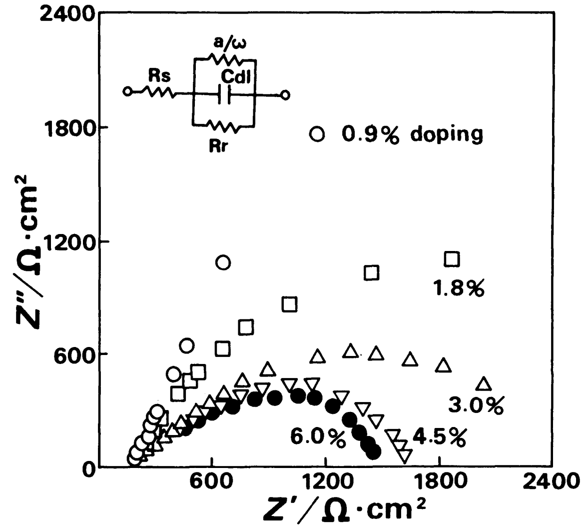

Fig. 2. Cell-impedance representation of charging process for Li-$(CH)_x$ battery step-by-step-charged at 0.5 mA cm^{-2}, where the cell impedance was measured after 24h at each doping level.

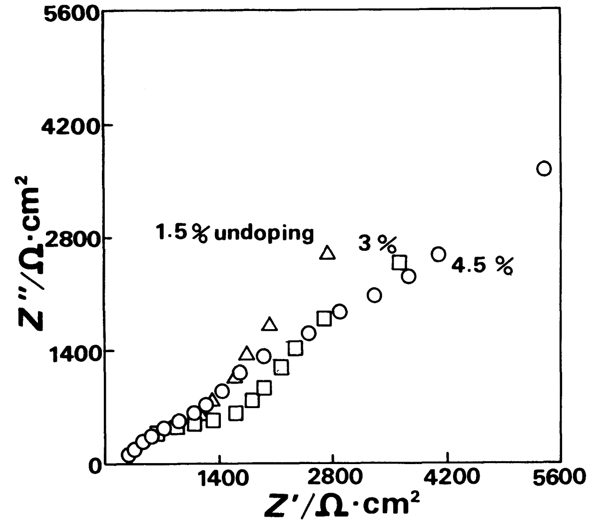

Fig. 3. Cell-impedance representation of the 6% ClO_4^- doped Li-$(CH)_x$ battery for discharging process at 0.5 mA cm^{-2}, where the cell impedance was measured after 24h at each undoping level.

The reduction of Li^+ to metallic Li occurs simultaneously:

$$Li^+ + e \longrightarrow Li. \qquad (2)$$

In our experiments, results identical to those in the previous papers[1,2] were obtained. In particular, the *Voc* decrease after charging and the *Voc* increase after discharging were clearly observed. For example, for the charging process, the *Voc*-charged values after 2h were always higher than those after 24h, while for the discharging process, the reverse was true. By considering the previously reported finding[2,3] that a quick charging process causes a nonequivalent concentration gradient of the doped ion in the $(CH)_x$ film for the depth profile, the above results can be interpreted by the facts that most of the ClO_4^- dopant exists near the surface region of the $(CH)_x$ film just after the charging process and, furthermore, that the dopant at the surface diffuses into the film interior with the passage of time. Thus, the *Voc* value is controlled by the dopant concentration at the surface. On the other hand in the discharging process, an immediate discharge produces a decrease in the dopant concentration at the surface region, but the passage of time after discharging process causes a increase in diffusion from the interior to the exterior parts of films.

Impedance Measurement of Charging-Discharging Process using Li-$(CH)_x$ Battery. The impedance-frequency dispersions for the Li-$(CH)_x$ at various charging levels were measured by the FFT impedance method. The cell-impedance representation for the battery galvanostatically charged step by step at 0.5 mAcm^{-2} is shown in Fig. 2. The cell-impedance measurement was done after 24h at each doping level. The cell-impedance representation becomes an inclined semicircle, like the behavior of the polyacetylene film itself.[3] Since two electrode reactions, (1) and (2), in the charging process occur simultaneously at the anode and the cathode respectively, the cell impedance should represent the whole reaction of the Li-$(CH)_x$ battery. However, the cell impedance can be regarded as mainly due to the polyacetylene electrode reaction (1), because the impedance due to the lithium-electrode reaction can almost be ignored because its value is lower than that due to the polyacetylene reaction (*i.e.*, the former reaction rate is faster than the latter). In practice, the semicircle impedance plots are somewhat distorted as compared with those of the $(CH)_x$ film itself,[3] so the influence of the Li-electrode reaction on the cell-impedance behavior may be somewhat contained. The Randles-type equivalent circuit shown in the insert of Fig. 2, which has already been discussed in a previous paper,[3] is applied to the frequency-dispersion behavior showing a semicircle. The components, *Rs*, *Rr*, *Cdl* and $a\ \omega^{-1}$ (ω: angular frequency), are the solution resistance, the resistive component due to the electrode reaction and the film conductivity, the double-layer capacitance, and the corrective term concerned with the surface roughness. The polyacetylene film surface may be porous, for it is composed of fibril units, so that the term concerned with surface roughness should be assumed, and the *Cdl* value becomes the total value of each pore's double-layer capacitance. In these components, the *Rr* value, which corresponds to the semicircle's diameter of impedance behavior, greatly reflects the change in the charging or doping level. Therefore, the charging process of the Li-$(CH)_x$ battery can be pursued and discussed in terms of the variation in the *Rr* value as well as that of the $(CH)_x$ film itself. The resistive component, *Rr*, arises mainly from the two factors of the partial oxidation (or doping) reaction and of the film resistivity itself; it

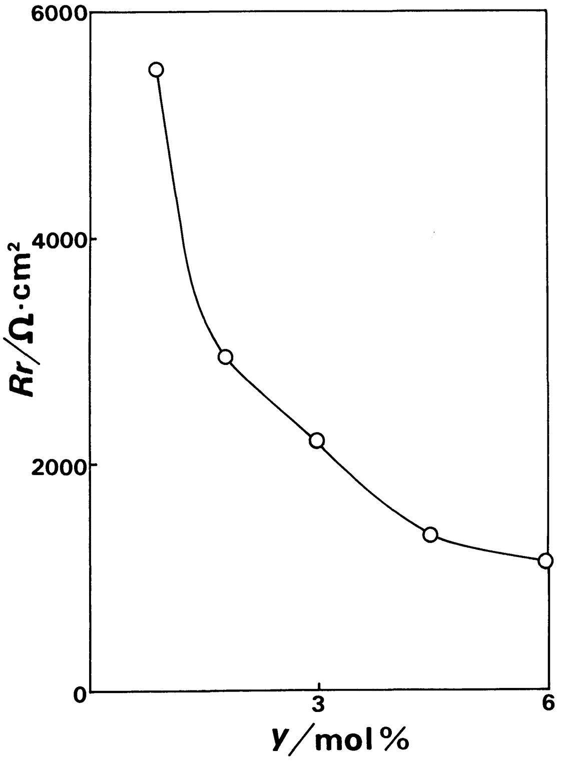

Fig. 4. Relation between resistive component, *Rr*, in the equivalent circuit and doping level, *y*, of the Li-$(CH)_x$ battery step-by-step-charged at 0.5 mA cm^{-2}, where the data were calculated from those in Fig. 2 at each doping level.

greatly reflects the dopant concentration not of the whole amount of the charge, but of the amount at the surface region of the $(CH)_x$ film, as is discussed in our previous paper.[3]

Figure 3 shows the cell-impedance representation for the discharging process of the Li-$(CH)_x$ battery at 0.5 mA cm^{-2} on various undoping levels from the 6% ClO_4^- doped polyacetylene. Each plot was also measured 24 h after the end of discharge. In the discharging process, there was observed to be no difference in cell-impedance behavior between measurements immediately after and 24 h later. Furthermore, the frequency-dispersion behavior of cell impedance is almost independent of the undoping level, as may be seen in Fig. 3. The cell-impedance behavior in the discharging process displays two regions of semicircles at higher frequencies and a linear line at lower frequencies. The linear region is usually concerned with the diffusion process, so the dopant diffusion at the interface is considered to be greatly concerned with and to control the discharging process of the Li-$(CH)_x$ battery.

Figure 4 shows a typical variation in the *Rr* value as a function of the doping level, *y*, on a step-by-step-charging process at 0.5 mA cm^{-2}, which is derived from the data in Fig. 2. The results indicate a good correlation between *Rr* and *y*; namely, the *Rr* value decreases with the increase in the doping level, *y*. The *Rr* decrease tends to change sharply at the initial doping stage.

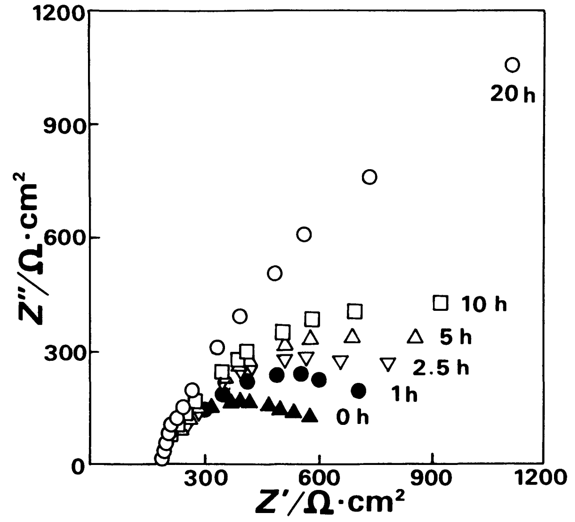

Fig. 5. Cell-impedance representation for self-discharge of Li-$(CH)_x$ battery after consecutive-charged at 0.1 mA cm^{-2}, up to the 6% ClO_4^- doping level.

Impedance of Self-discharge for the Li-$(CH)_x$ Battery after Consecutive Charging up to the 6% ClO_4^- Doping Level. Since the self-discharge phenomenon was observed after charging the ClO_4^- doped Li-$(CH)_x$ battery, the time dependence of impedance for the battery after it had been charged up to the 6% doping level was examined in order to clarify this phenomenon.

Figure 5 shows the cell-impedance representation of the self-discharge of the Li-$(CH)_x$ battery after it has been charged at 0.1 mA cm^{-2} up to the 6% ClO_4^- doping level. The frequency dispersion of the impedance loci becomes a semicircle, just as in Fig. 2. Similar the cell-impedance behavior was also observed in the cases of the 0.2 and 0.5 mA cm^{-2} charging currents. The *Rr* value in the equivalent circuit, corresponding to the semicircle's diameter in the cell-impedance representation, increases with the passage of time. These results can be explained by the fact that the dopant diffuses from the exterior into the interior parts of the $(CH)_x$ film with the increase in time, as well as by the *Voc* results previously discussed.

Figure 6 presents the time dependence of the resistive component, *Rr*, and the open-circuit voltage, *Voc*, for the self-discharge of the Li-$(CH)_x$ battery after it has been charged up to the 6% ClO_4^- doping level. The *Rr* value shown in Fig. 6a increases with an increases in the time after the charging process, finally reaching the maximum constant value of *ca.* 3500 Ωcm². The time required to reach the maximum constant value, *tm*, becomes longer with the increase in the charging-current value. This indicates that the dopant diffusion into the $(CH)_x$ film occurs until it reaches a dopant-concentration equivalent to the 6% doping level, whose state is established after the *tm* value, and also that the lower charging-current value produces the more uniform doping state. The behavior of the *Voc* value

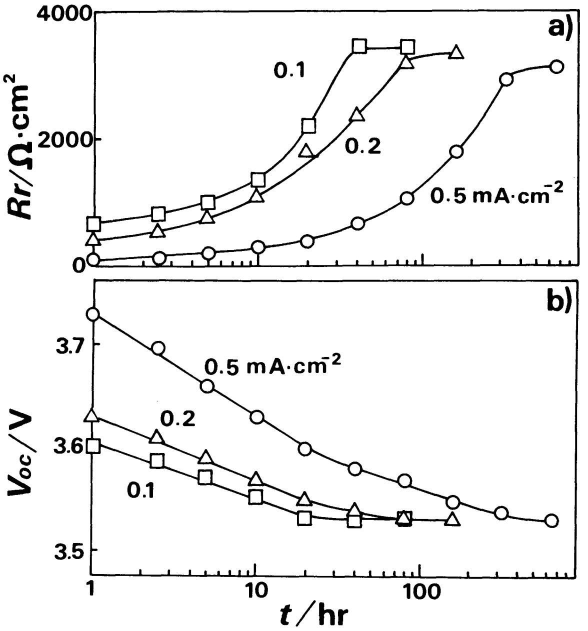

Fig. 6. Time dependence of resistive component, *Rr*, and open-circuit voltage, *Voc*, for self-discharge of Li-$(CH)_x$ after consecutive-charged at various current densities up to the 6.0% ClO_4^- doping level.

shown in Fig. 6b displays almost the same trend as that of the *Rr* value in Fig. 6a; that is, the *Voc* value gradually decreases with the passage of time, finally reaching the almost constant value of 3.53 V. The higher charging current makes the *tm′* (the time required to reach a constant *Voc*) longer at the same 6% doping level. The time, *tm*, in the *Rr-t* relation corresponds nearly to the time, *tm′*, in the *Voc-t* relation. The *Voc* value is entirely almost determined by the dopant concentration at the $(CH)_x$ surface[1,2], thus, it may be concluded from the dependence of *tm* or *tm′* on the charging current that the higher charging current produces the higher dopant-concentration gradient for the depth profile, and, furthermore, that the doping states in the $(CH)_x$ film can be evaluated sensitively from the *Rr*-value behavior.

Since the correlation between *Rr* and *Voc* can be presumed from the data in Fig. 6, the relation between *Rr* and *Voc* obtained by the time dependence of *Rr* and *Voc* after charging up to the 6% doping is obtained as shown in Fig. 7. In Fig. 7, there are two kinds of data for the self-discharge process after consecutive charging up to the 6% ClO_4^- doping level, calculated from the data in Fig. 6, and for the step-by-step-charging process from the 0.9 to the 6% doping level, calculated from the data in Fig. 2. For the self-discharge process, there clearly appears a correlation between *Rr* and *Voc*, regardless of the charging current. The *Voc* for the self-discharge process becomes close to the equivalent value of *ca.* 3.5 V for the 6% doping level regardless of the charging current. The *Voc* value higher than 3.5 V clearly means that the doped-ion-concentration gradient occurs at the surface. For the step-by-step charging, the same *Rr* value as that for the self-discharge process correlates with the lower *Voc* value, and the final *Voc* value at the 6% doping level shows the equivalent value of *ca.* 3.5 V, so that the slow step-by-step charging is suitable for uniform doping with no occurrence of the higher dopant-concentration gradient producing the self-discharge. Finally, the *Rr* value after the charging process not only reflects closely the doping states of the $(CH)_x$ film, but can also be used to investigate the self-discharge conditions of the Li-$(CH)_x$ battery.

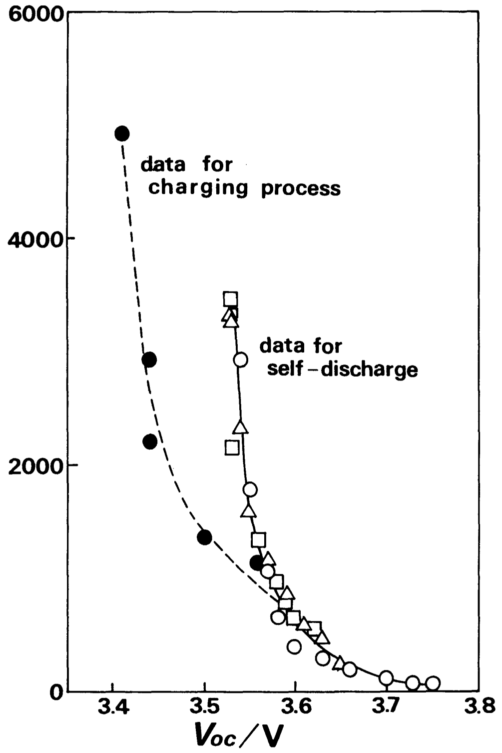

Fig. 7. Relation between resistive component, *Rr*, and open-circuit voltage, *Voc*, for self-discharge after consecutive-charged up to the 6.0% ClO_4^- doping level (*cf.*, Fig. 6), and for step-by-step-charging process (*cf.*, Fig. 2).
○: 6.0% doped at 0.5 mA cm^{-2}, △: 0.2 mA cm^{-2}, □: 0.1 mA cm^{-2}, ●: 0.9—6.0% stepwise-doped at 0.5 mA cm^{-2}.

Conclusion

Charge-discharge and self-discharge characteristics of the ClO_4^- anion-doped lithium-polyacetylene battery were studied by means of the FFT impedance measurement. The impedance-frequency dispersion for charging and self-discharging of the battery was basically interpreted by the Randles-type equivalent circuit. The conditions of the charged battery and the self-discharge were strongly correlated to the resistive component, *Rr*, in the equivalent circuit. The discharging process was observed to behave differently from the charging process. In conclusion, the nonequivalent states of the doped-ion-concentration gradient of the polyacetylene film were readily checked by the *Rr* component, and the large self-discharge phenomenon was produced by the nonequivalent states of the doped ions.

The authors would like to thank Mr. Yoshimitsu Sawada, Showa Denko Co., Ltd., for providing the polyacetylene samples and for his valuable discussion.

References

1) P. J. Nigrey, D. MacInnes Jr., D. P.Nairns, and A. G. MacDiarmid, *J. Electrochem. Soc.*, **128**, 1651 (1981).
2) K. Kaneto, M. Maxfield, D. P. Nairns, and A. G. MacDiarmid, *J. Chem. Soc., Faraday Trans.*, **78**, 3417 (1982).
3) T. Osaka and T. Kitai, *Bull. Chem. Soc. Jpn.*, **57**, 759 (1984).
4) T. Osaka and K. Naoi, *Bull. Chem. Soc. Jpn.*, **55**, 36 (1982).
5) Y. Ito, H. Shirakawa, and S. Ikeda, *J. Polym. Sci.*, **12**, 11 (1974).
6) Y. Matsuda, *Denki Kagaku*, **48**,665 (1980).